Chapter 6
Exemplary Application

The developed multiscale simulation concept is exemplary applied to two different battery production systems. The purpose of this application is demonstrating the use of the simulation concept, the core model, the development of detailed models, as well as the interpretation of simulation results. Since the simulation is applicable for all production stages and different objectives, the application is demonstrated for cell production (Sect. 6.1) as well as for the assembly of battery modules (Sect. 6.2).

6.1 Simulation of Cell Production

In the first study, a simulation model was created for the production of LIB cells at the Battery LabFactory Braunschweig (BLB). The twelve-step application procedure for multiscale simulations structures the following subsections.

6.1.1 Problem Formulation (I) and Objective Definition (II)

The BLB is a battery cell research facility.[1] It serves as a platform for interdisciplinary research on the process chain for electrodes and cells. Research fields are cell design, process improvement, sustainable manufacturing, battery cell and production system simulation, as well as data acquisition and knowledge discovery in production. The BLB is equipped with state-of-the-art production equipment such as different types of

[1] The BLB was established in 2013 at the Technische Universität Braunschweig as an institution of the Automotive Research Centre Niedersachsen (NFF); www.tu-braunschweig.de/blb.

M. Schönemann, *Multiscale Simulation Approach for Battery Production Systems*,
Sustainable Production, Life Cycle Engineering and Management,
DOI 10.1007/978-3-319-49367-1_6

mixers, a continuous coating and drying machine, a calender, a laser cutter, automated machines for cell assembly, and cycling automates. The assembly of cells at the BLB is located inside a 150 m^2 dry room and is characterized by small batch sizes and manual handling operations.

The objective of the simulation is imitating the operation of the BLB – under the assumption that it operates at full capacity – and to demonstrate the capabilities of the proposed multiscale simulation approach. The simulation shall determine performance indicators such as the output of cells per time period and the utilization of equipment, as well as energy demands for different scenarios. More specifically, the simulation shall enable the evaluation of the impacts of machine configurations, processing times as well as different materials on the energy demand. In addition, the simulation shall allocate the energy demands to produced cells and create transparency about the pattern of energy demands in order to identify the most relevant machines and systems. The goal was to demonstrate the interaction of different models as well as possible results and use cases of the multiscale simulation.

6.1.2 Definition of Required Models (III)

The multiscale core model was used to simulate the material flow and to determine the operation and demands of machines. This allows the coordination of detailed models. In order to configure the core model and to define the required machine agents, machines and peripheral equipment have been analyzed. According to the proposed decision tree for model type selection, the machines of the process chain must be included in the simulation. Detailed modeling of machines or equipment may be reasonable if the energy demand is high and volatile see (Sect. 4.7.3). Hence, machines and equipment were observed regarding power demands and operational time to derive the required type of modeling for each equipment. The results of a portfolio analysis provided by Posselt (2016) were used as a starting point for the identification of machines/systems with high energy demands. In addition, an analysis of measured load profiles of machines and equipment was carried out to gather detailed insight into demand patterns. As a result, the following machines and systems have been identified to have high energy demands:

- continuous coating and drying machine
- calender
- cycling automate
- extruder
- ventilation units incl. heating and cooling
- dry room units
- chiller

These machines and systems were further investigated to determine whether the power demands are volatile and require detailed modeling or if generic models provide sufficient accuracy. As an example, the power demand of the calender was

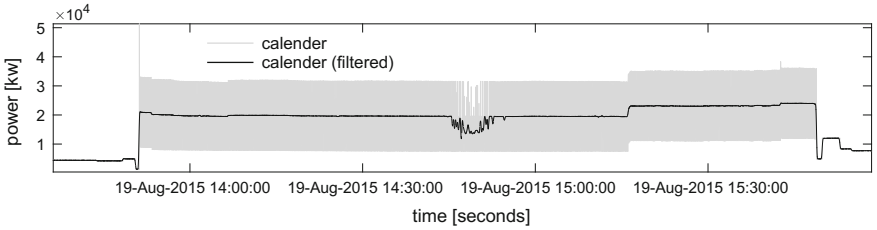

Fig. 6.1 Power measurement of calender. Unfiltered and filtered data

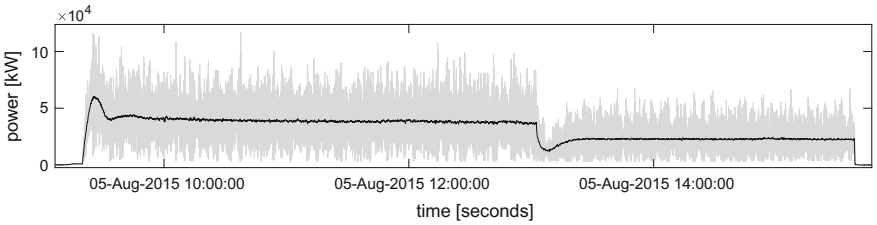

Fig. 6.2 Power measurement of coating and drying machine. Unfiltered and filtered data

examined and the power demand profile – presented in Fig. 6.1 – shows rather constant power demands for idling and processing. Generic modeling seams reasonable.

As another example, Fig. 6.2 shows a characteristic power demand profile of the coating and drying machine. During ramp-up, the power demand increases until the desired drying temperature is reached. The power demand remains constant during processing and drops to a lower level at which it stays constant again. This allows to conclude that the power demand during processing depends on process parameters. Overall, the power demand of the coating and drying machine could be simplified modeled by a generic machine model in which the state-based power demand depends on process parameters. However, if NMP solvent is used in the electrode slurry, this solvent is emitted in the drying process and the exhaust air has to be filtered before it leaves the building. A treatment system is required which consists of components with high power demands. It has to be modeled and connected to the dryer model in order to simulate the effects of different solvents on the energy demand.

This analysis approach was used for all other machines and equipment with high energy demands. It revealed that all selected machines can be sufficiently modeled with generic models due to constant power demand profiles. There are also machines with higher variation in power demand such as the z-folder or the laser cutter. However, their overall power demand is relatively low which means that a state-based modeling approach with average values is reasonable for a first estimation of the production systems energy demand. Detailed models of these machines may still be reasonable if it is desired to simulate the impacts of machine behavior on process results. For example, the speed of a gripper in the z-folder may effect the positioning accuracy of electrodes. To investigate these effects, a detailed machine model of the

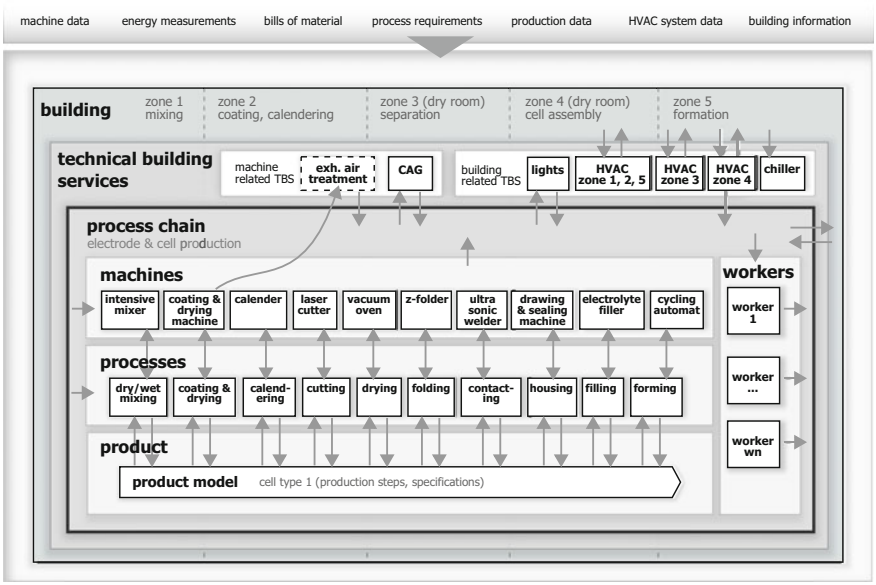

Fig. 6.3 Framework for the multiscale simulation of the BLB

z-folder with each component was created in the software Simulink with defined variables for the connection to the core model. However, these aspects and the model were neglected.

The defined models and their relations must be clearly structured within the context of the multiscale simulation. This can be realized by using the suggested framework for multiscale simulation. Figure 6.3 presents the adapted framework for the simulation of the BLB.

6.1.3 Modeling, Implementation (IV), and Coupling of Models (V)

The defined models have to be further specified and implemented in software. The core model, the compressed air system model, and the machine models have to be configured. In addition, detailed models have to be created for the HVAC systems including the dry room and a model for the building zones.

Multiscale Core Model

The multiscale core model was configured to represent the BLB. This required the definition of product types, material flows, jobs, machines, and building zones. An image of the building ground plan was placed in the background of the models main level and zones were defined based on the actual building zones. The machine

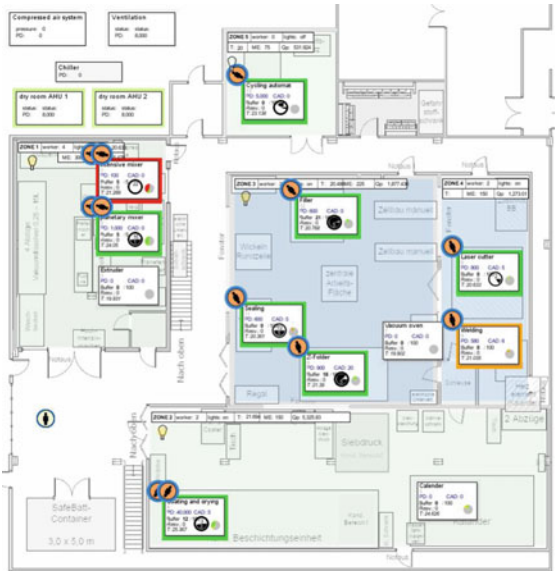

Fig. 6.4 Screenshot of the multiscale core model implemented in Anylogic during a simulation run

location was specified within the shop floor coordinates according to their position in the ground plan. This allows an easy interpretation of the dynamic model behavior and results during simulation. Figure 6.4 shows a screenshot the process chain model representation of the BLB. The machines are modeled with the machine agent class provided by the process chain model. Each machine was configured based on machine specific parameters and state-based energy and compressed air demands.

As an example for an extended machine model, the coating and drying machine was modeled in more detail to describe the effects of process parameters and the operation of the exhaust air treatment system. This model was implemented in AnyLogic within the machine agent class. The state-based power demand values for the machine were derived from empirical results. Measurements were taken and examined for various process parameter combinations. The analysis revealed that the power demand is mostly effected by the dryer temperature. Figure 6.5 shows box plots of the power demand of the machine for the temperatures 80, 100, and 120 °C. Within the model, the power demand is adjusted based on a defined temperature. Furthermore, the air treatment system was modeled with state charts describing the main components fan, filter, and chiller.[2]

[2]The fan has a nominal power of 11 kW but it mostly operates at 30% of this power. The filter requires compressed air. The purpose of the chiller is cooling of the exhaust air before entering the filter. The chiller has a nominal power of 65 kW. Its power demand depends on the outside air temperature. Since no exact energy data exist so far, a template for a function was implemented which can initially be used for a rough estimation of the chiller power demand and later be adapted.

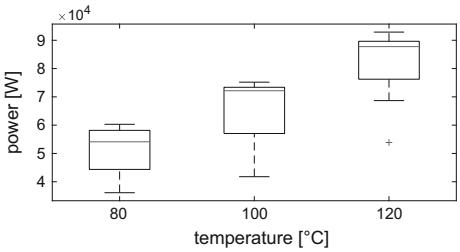

Fig. 6.5 Power demands of continuous coating and drying machine for three different drying temperature settings

The control strategy of the process chain had to be adjusted to account for aspects of the small scale production. It is assumed that production activity starts at 7 am and stops at 8 pm on each day (including weekends). The cycling automate is the only machine running at night. All other machines start processing only if the processing time is shorter than the remaining shift time. Furthermore, the mixing process only starts if the slurry can be used for coating at the same day. The buffer capacities at each machine are set high in order to avoid blocking. Mixers and the coating and drying machine have small buffers since they have to be immediately available at the beginning of a job.

Since battery production is highly automated, the influences of worker performance on product quality were neglected within this study.[3]

Building and HVAC Model

The BLB has five building zones. Zone 1 contains the mixing processes and is ventilated, heated, and cooled. Zone 2 contains the coating and drying machine and the calender. It is ventilated and heated. Zone 3 and 4 are dry rooms for cell assembly. Zone 5 contains the cycling automate and is ventilated and heated.

For simulation of the building inside conditions, a simplified five room model was built in Simulink using the International building physics toolbox (IBPT).[4] Each zone was composed using construction objects for walls, windows, ceilings, as well as ventilation and air conditioning systems. Weather data were prepared based on TRY-files for Germany (DWD 2016). Figure 6.6 shows a screenshot of the building zone model. In the model, each building zone is ventilated with a constant air change rate and power demands for ventilation are assumed to be constant within each of the states operation and standby according to measurements taken at the BLB.[5] The heating energy is supplied to the BLB as district heat. In addition to the supplied heat, the process chain model determines heat emissions of machines, lighting, and

[3] It is possible to implement existing worker performance models (e.g. from Baines et al. 2004) into a multiscale simulation if the results are expected to be beneficial.

[4] The open-source toolbox was developed by the Building Physics research group of the Chalmers University of Technology in Gothenburg, Sweden and the Department of Civil Engineering from Technical University of Denmark in Copenhagen. The resources and information are available on www.ibpt.org.

[5] For each zone: 8 kW in operation and 5 kW in standby mode.

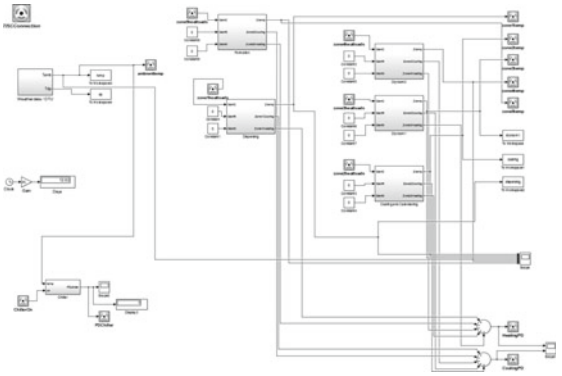

Fig. 6.6 Five-zone building model implemented in Simulink

workers to each building zone. These heat emissions reduce the required heat supply and may demand cooling. The building model determines the resulting heating and cooling power demand required to maintain zone temperatures between 20 and 26 °C. The simulated heating demand equals the district heat demand[6] while the cooling demand has to be provided by a chiller.[7]

The dry rooms are both supplied by an AHU each containing fans, cooling coils for pre-cooling of the outside air (supplied by the chiller), a desiccant wheel, a heating coil for heating of the dried air to the desired room temperature (district heating), a heating coil for the regeneration air flow (gas), and a waste heat recovery from the regeneration air. In order to estimate the power demand of the dry room operation, a model is derived based on power measurements[8] and the analysis of the control scheme. First measurements have shown a rather constant gas demand[9] during dry room operation as well as a constant power demand for ventilation. In addition, a regression analysis was conducted to investigated the correlation between the outside temperature and the power demand of the chiller. Figure 6.7 shows a scatter plot of samples for the power demand during intervals with an average temperature. It also shows a fit based on a polynomial function, which was implemented in the chiller model to estimate the power demand depending on the outside temperature.[10]

The effects of moisture emissions of workers and the relative humidity of the outside air on the energy demand of the dry room components were not considered. However, due to the structure of the dehumidification system, it is assumed that

[6]It was assumed that heat supply is available throughout the entire year although it might be turned off during summer months.

[7]The model determines the required cooling demand to maintain the zone temperature in the desired range. However, in the BLB, the capacity of the available chiller is not large enough to supply the dry room AHU as we as to provide cooling for all zones.

[8]Measurements were only available for April, August, September and October.

[9]Approximately 7 m^3/h. However, due to the lack of sufficient data, this aspect is neglected in the model so far.

[10]Goodness of fit: R-square: 0.8496. The quality of this fit has to be re-evaluated if more data samples are available.

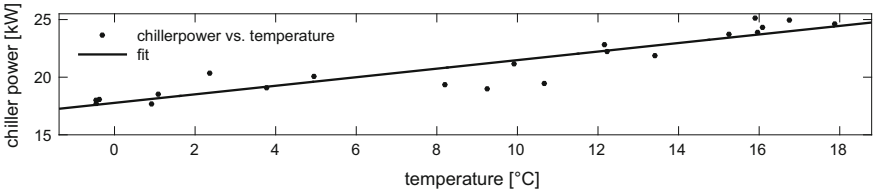

Fig. 6.7 Scatter plot of samples of chiller power demand [kW] and outside air temperature (°C)

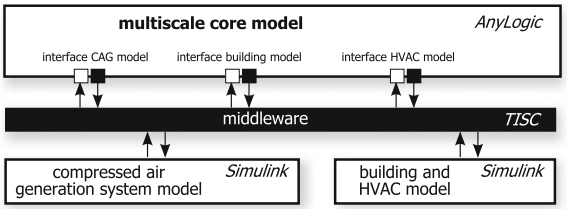

Fig. 6.8 Model coupling structure

higher internal moisture loads and higher outside air humidity would result in a higher gas demand.[11] Moreover, in addition to the use of constant values (e.g. as for the ventilation power demand) or empirical model (e.g. as for the chiller power demand), it is also possible to calculate the theoretical energy demands based on the specific characteristics of the air streams to and from the dry room. Such detailed modeling may be reasonable for system or control design or to accurately determine the indoor conditions. However, it would require further in-depth knowledge about the dehumidification and ventilation system and cause higher modeling effort.

Model Coupling

The building model and the compressed air system model are connected to the core model via the middleware TISC, as shown in Fig. 6.8. The building model receives information from the process chain model about the shift schedule and variables about heat emissions for each building zone. In return, the building model provides the temperatures for each zone, the heating and cooling demands, as well as the power demand of the chiller. The zone temperatures are used in the core model to calculate the heat emissions of each machine. Furthermore, the building model provides the outside air temperature which is used to determine the power demand of the chiller of the air treatment system.

[11] Further studies could deal with the measurement of the zone dew point temperature along with the number of people inside a dry room over a time period. This may enable to derive a regression function for the power demand depending on moisture loads.

6.1.4 Verification and Validation (VI)

The general verification of the core model, the compressed air system model, and the coupling via TISC was already explained in the previous chapter. The models used in this study were verified based on available production data and energy measurements. Since the BLB is usually not operating at full utilization, data about energy demands and control of HVAC systems are not completely available. Furthermore, the building and HVAC model was modeled without having complete data and information about system characteristics and control parameters. As an example for limitations, heat transfers between building zones are not considered and the materials of construction elements are not exactly matched with the materials used in the BLB. Moreover, the calculation of humidity is not included in the building model. However, the geometry of building zones is specified accurately and the model in general shows the expected thermal behavior. For example, the temperatures in larger zones change slower compared to zones with smaller air volume and zone temperatures increase if heat is emitted from internal heat sources (provided by the core model). Thus, the simulation results are useful as a rough estimation of the building climate and to highlight the directions of interdependencies between model parameters. In summary, although some models were verified and validated based on available data, the overall model cannot be considered validated and serves only as an experimental model demonstrating the functionality of the multiscale simulation.

6.1.5 Definition (VII) and Execution (VIII) of Simulation Runs

Specific simulation runs have to be defined based on the objectives and models have to be configured accordingly. In this study, different experiments are used to illustrate possible use-cases of the multiscale simulation. First, a reference scenario is defined which imitates one month of production of one type of battery cells. Jobs, product types, processing parameters, machine allocation and processing times were defined in order to create a consistent scenario of the cell production within the BLB.[12] Each job represents the production of 50 cells and it is assumed that one anode batch and one cathode batch are used for exactly these 50 cells. This reference scenario can be used as a benchmark to evaluate the effects of different system changes related to various planning tasks. This case study addresses the following five exemplary tasks:

T_1: Evaluation of different drying times and temperatures The coating and drying machine has a high power demand and relatively long processing times. It can be assumed that this machine is a bottleneck which effects the output of

[12]Since there is no established series production scenario of the BLB, this reference scenario represents one exemplary system configuration which is not necessarily completely representative for the BLB.

cells and causes high energy demands. It should be evaluated how the output and energy demand is effected by different processing times and temperature settings.

$\mathbf{T}_2$: **Evaluation of additional machines** The reference scenario refers to the actual machine configuration of the BLB. However, since the BLB is not equipped for series production, it is expected that the material flow will be blocked and that buffers will run full due to limited capacity of some processes. For this reason, the simulation should enable evaluating if additional machines can improve the material flow and increase the output.

$\mathbf{T}_3$: **Evaluation of different solvents** Electrode slurries can contain different solvents. Often NMP is used which is removed within the drying process and requires treatment of the exhaust air. If water is used as solvent, no air treatment is necessary. The effects of solvents on energy demands should be evaluated.

$\mathbf{T}_4$: **Evaluation of different weather conditions** The reference scenario is simulated with weather data for July. It is of interest to evaluate how much the HVAC energy demands are effected by the outside air temperature.

These evaluation tasks are the basis for the derivation of simulation runs. Simulation runs represent scenarios with different production system and simulation model configurations. They have to be specified to generate simulation results which allow the evaluation of the related tasks. Table 6.1 lists the description of defined simulation runs for this case study. These runs have been executed to generate results.[13]

Table 6.1 Description of simulation runs

SR	Description
SR_{RS}	Simulation run for the reference scenario
$SR_{1,1}$	Reference scenario but with drying time increased by 10%
$SR_{1,2}$	Reference scenario but with drying time increased by 20%
$SR_{1,3}$	Reference scenario but with drying time reduced by 10%
$SR_{1,4}$	Reference scenario but with drying time reduced by 20%
$SR_{1,5}$	Reference scenario but with temperature at 100 °C
$SR_{1,6}$	Reference scenario but with temperature at 120 °C
$SR_{2,1}$	Reference scenario but with two filling machines
$SR_{2,2}$	Reference scenario but with two coating and drying machines
$SR_{2,3}$	Reference scenario but with two filling machines and two coating and drying machines
$SR_{3,1}$	Reference scenario with slurry containing NMP solvent. Air treatment system is activated
$SR_{3,2}$	Machine configuration from $SR_{2,2}$ with slurry containing NMP solvent. Air treatment system is activated
$SR_{4,1}$	Reference scenario but with weather data for January
$SR_{4,2}$	$SR_{2,3}$ but with weather data for January
$SR_{4,3}$	Reference scenario but with weather data for October
$SR_{4,4}$	$SR_{2,3}$ but with weather data for October

[13] Each run starts with empty buffers and consequently not in steady state. In addition, stochastic effects such as machine failures or process variations are neglected due to the lack of required data.

6.1.6 *Evaluation of Simulation Results (IX) and Objectives (X)*

The results of the simulation runs were examined regarding result quality and usability for the evaluation of the defined tasks. Figure 6.9 presents exemplary plots of performance indicators of $SR_{2,3}$ for the simulation period of one month. These plots show (from top to bottom) the power demands of machines, compressed air generation, heating and cooling, the dry room (ventilation and chiller), and lighting. These plots enable identifying trends and characteristic situations. For example, a daily power demand pattern can be identified from the first plot. Furthermore, heating demands are higher at times with lower outside temperature and cooling is only active during days with a higher outside temperature. In addition to these monthly plots, it is possible to visualize the total energy demand of each machine and system for the simulated month – as shown in Fig. 6.10 for $SR_{2,3}$. This visualization helps to identify the most relevant machines/systems. Here it becomes clear that the highest energy demands are caused by building cooling demand, coating and drying machines, the chiller for the dry rooms, as well as the ventilation of zones.

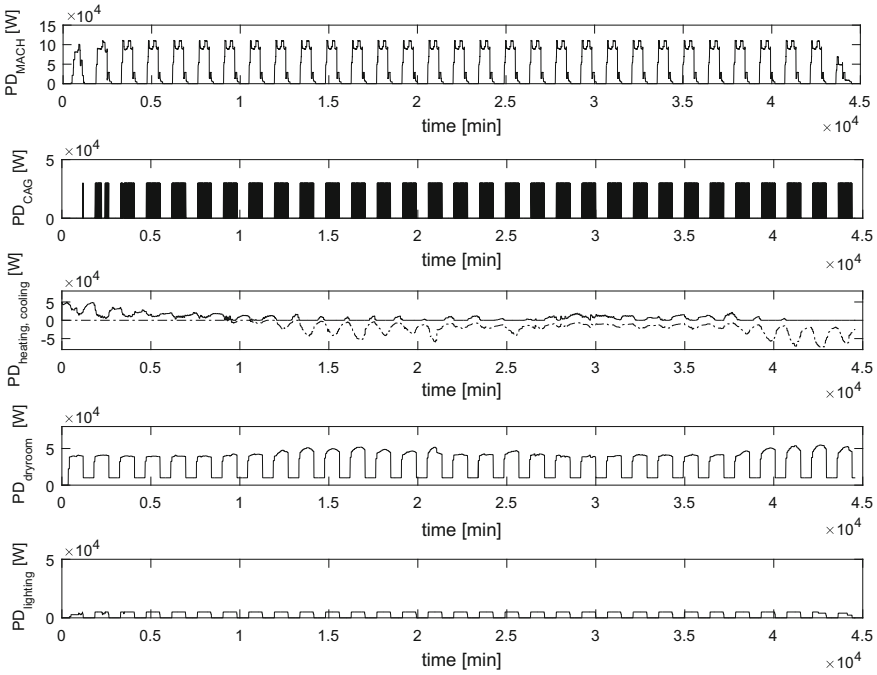

Fig. 6.9 Plots of indicators for $SR_{2,3}$. From *top* to *bottom*: power demand of machines, compressed air generation, heating and cooling, dry room, and lighting

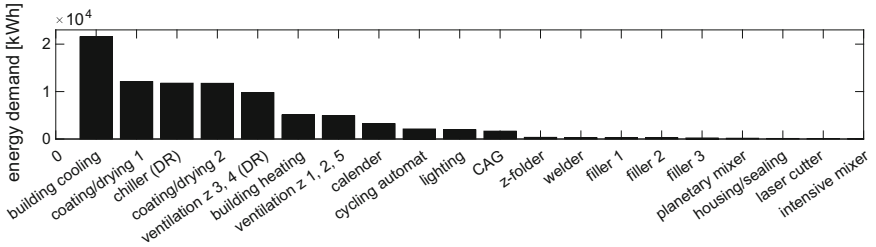

Fig. 6.10 Energy demands of machines and systems during one month for $SR_{2,3}$

In this case study, indicators have been selected for the comparison of simulation runs. These indicators were the yield of cells during the simulated period of one month, the utilization of the process chain (uti_{PC}), the mean production time per job (PT_{mean}) and its deviation (PT_{dev}), energy demands (ED) of different systems, as well as the average direct and indirect embodied energy per cell ($\varnothing$ DEE_{cell}, $\varnothing$ IEE_{cell}). Table 6.2 lists the results for the simulation runs. Even though the actual numerical values of the results must be doubted due to the non-validated model character, they enable a discussion of the individual measures, the comparison of simulation runs, and the improvement of the understanding of the complex behavior of the production system.

The results of the reference scenario SR_{RS} show that the mean of the production time per job is high with 189 h. A detailed analysis showed that the production time increased over the observed time period. This is caused by including the model warm up phase into the simulation results. After reaching a steady state, the model shows that the machines in cell assembly have full buffers because the filling process is a bottleneck. Many semi-finished product units are stored in buffers and cannot be finished due to limited machine capacities. Furthermore, the mixing processes are often blocked which allows to conclude that the coating and drying machine is also a bottleneck. However, the sole extension of coating and drying capacities would only result in more buffered semi-finished product units in cell assembly. In summary, the high mean production time indicates a large amount of work in progress and an undesired obstructed material flow.

The results of $SR_{1,1}$–$SR_{1,4}$ show the effects of different processing times for coating and drying. As expected, longer processing times result in higher energy demands of machines and higher direct embodied energy per cell. The reduced mean production time of $SR_{1,2}$ compared to $SR_{1,1}$ can be explained with fewer started jobs due to not available coating capacities. Thus, fewer product units fill the buffers in cell assembly causing shorter production times. The opposite effect shows in $SR_{1,4}$: A shorter time for coating and drying increases the yield because the cell assembly can start earlier within the simulated month. On the downside, higher throughput in electrode production fills the buffers in cell assembly more quickly causing the production times to increase even more for later jobs and blocking of the previous processes. The resulting reduced activity in electrode production results in lower

Table 6.2 Results of simulation runs

SR	Yield	PT_{mean} (h)	PT_{dev} (h)	ED_{TOTAL} (kWh)	ED_{MACH} (kWh)	ED_{CAG} (kWh)	ED_{HVAC} (kWh)	ED_{LIGHTS} (kWh)	∅ DEE_{cell} (kWh)	∅ IEE_{cell} (kWh)
SR_{RS}	1129	189	58.9	57,003	17,030	878	36,760	1,905	11.292	39.198
$SR_{1,1}$	1129	189	58.8	58,272	18,303	873	37,218	1,877	11.995	39.619
$SR_{1,2}$	1107	186	53	59,146	18,949	863	37,478	1,854	12.973	40.455
$SR_{1,3}$	1129	189	59	55,166	15,907	887	36,501	1,870	10.583	38.28
$SR_{1,4}$	1136	249	109	54,333	14,627	1,014	37,079	1,612	10.466	37.362
$SR_{1,5}$	1129	189	59	72,675	28,639	878	41,253	1,905	17.008	47.634
$SR_{1,6}$	1129	189	59	81,654	34,570	878	44,300	1,905	20.223	52.101
$SR_{2,1}$	1485	96	14	55,268	16,156	868	36,645	1,589	10.342	26.875
$SR_{2,2}$	1140	292	137	57,919	17,095	1,039	38,348	1,435	11.878	38.928
$SR_{2,3}$	2845	87	13.5	78,106	30,885	1,665	43,660	1,934	9.91	17.543
$SR_{3,1}$	1129	189	59	66,593	26,880	1,049	36,759	1,905	16.675	42.309
$SR_{3,2}$	1485	96	14	65,324	26,013	1,037	36,661	1,611	15.93	28.06
$SR_{4,1}$	1129	189	59	101,392	17,029	878	81,579	1,905	11.292	78.516
$SR_{4,2}$	2845	87	13.5	103,756	30,885	1,655	69,310	1,934	9.91	26.56
$SR_{4,3}$	1129	189	59	73,433	17,029	878	53,620	1,905	11.292	53.751
$SR_{4,4}$	2845	87	13.5	64,746	30,885	1,655	46,547	1,934	9.91	17.947

overall energy demands while maintaining a similar yield compared to the previous simulation runs. However, the amount of produced electrodes is lower at the end of one month.

$SR_{1,5}$–$SR_{1,6}$ differ from the reference scenario only regarding the power demand for the coating and drying machine. The results show the expected higher energy demand of machines but also of HVAC systems due to higher cooling demands. Consequently, the direct and indirect embodied energy per cell is effected noticeably by the drying temperature.

$SR_{2,1}$–$SR_{2,3}$ examined the impacts of additional machines. First, in $SR_{2,1}$, two additional filling machines resulted in a higher yield due to a resolved bottleneck at the end of the process chain. The mean production time dropped significantly. The utilization of cell assembly was reduced (since buffers were not always filled and machines were in idle mode) which can be seen at the reduced power demand for compressed air generation. As a result of the higher yield, the indirect embodied energy per cell was noticeably reduced because the fixed power demands could be allocated to more cells. In $SR_{2,2}$, the reference scenario was extended by a second coating and drying machine. The results indicate that the bottleneck was not eliminated since the mean production time is very high and the yield similar to the reference case. In $SR_{2,3}$, the reference scenario was extended by both two additional filling machines and one additional coating and drying machine. The results show that a higher yield and shorter production times were possible in this case. This underlines that the cell assembly was not fully utilized in $SR_{2,1}$.

The results of $SR_{3,1}$ show – in comparison to the reference scenario – that the air treatment system caused higher overall energy demand as well as higher direct (increased by almost 50%) and indirect embodied energy per cell. $SR_{3,2}$ revealed – based on $SR_{2,1}$ – that a higher output did not help to reduce the embodied energy since the energy demands of the air treatment system were assigned to the coating machine. If the energy demand of the air treatment system would have been allocated to the TBS systems, the higher output in $SR_{3,1}$ would have resulted in reduced indirect embodied energy compared to $SR_{3,1}$. It can be concluded that avoiding NMP solvents is an important measure in reducing the overall energy demand.

$SR_{4,1}$ and $SR_{4,2}$ used weather data for January. The high required heating demands caused an increase of the total energy demand and indirect embodied energy per cell. Even though the output of $SR_{4,2}$ is higher, the indirect embodied energy is still significantly higher compared to $SR_{2,3}$. $SR_{4,3}$ and $SR_{4,4}$ used weather data for October. The weather conditions caused lower heating and cooling demands due to moderate temperatures.

The embodied energy per battery cell is an important indicator for the evaluation of the environmental impacts of each cell. Figure 6.11 presents the simulation results for the average direct (DEE) and indirect (IEE) embodied energy of one battery cell. It becomes clear that the indirect embodied energy was higher in all simulation runs. Furthermore, the indirect embodied energy strongly depends on the yield of finished cells. This means that the energy demands of peripheral equipment and TBS as well as the yield of a factory must be considered in the economic and environmental assessment of battery cells. Moreover, the simulation results allow a breakdown

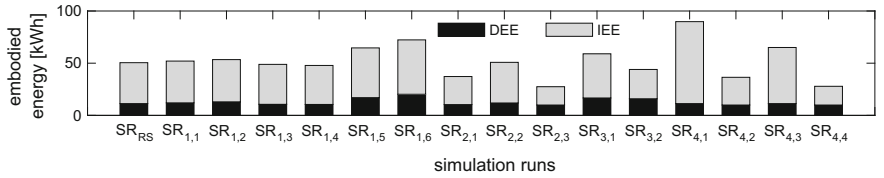

Fig. 6.11 Average direct (DEE) and indirect (IEE) embodied energy per battery cell

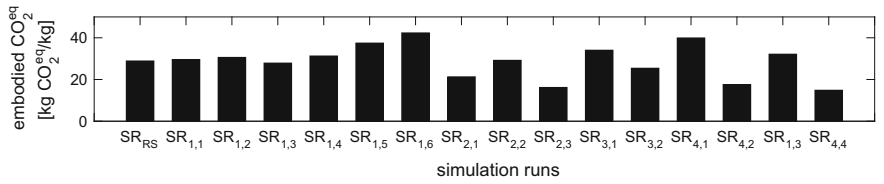

Fig. 6.12 Average embodied equivalent CO_2 emissions from energy supply per battery cell

of the energy demand into different energy carriers. This enables a more accurate determination of environmental impacts and energy costs. For example, in this study the building heating is supplied by district heat while the other machines and TBS systems demand electricity. These energy carriers cause different specific equivalent CO_2 emissions[14] which can be used to determine the average embodied equivalent CO_2 emissions from energy supply for each produced battery cell, as shown in Fig. 6.12.

In summary, the results allow to draw some general conclusions. The processing times of individual processes may effect the bottleneck(s) of a process chain and influence the achievable yield of finished cells. This further influences the indirect embodied energy per cell. Moreover, the energy demands of processes may depend on product specifications (e.g. type of solvent) and process parameters (e.g. temperature settings). As an example, the usage of NMP solvent increases the energy demand noticeably ($SR_{3,1}$ and $SR_{3,2}$). This also effects the direct embodied energy per cell. In addition, weather conditions have a significant effect on the energy demand of HVAC systems. Thus, weather conditions have to be considered while selecting a location for a battery cell factory.

Overall, the developed models can be used to conduct simulation runs for further planning tasks or for in-depth sensitivity analysis of single parameters or model characteristics. Moreover, the model functions allow the analysis of worker behavior, value streams of jobs, the development of product characteristics, etc. These aspects were not included in this case study but could be used for future studies.

[14] For Germany: CO_2^{eq} impact of electricity production: 609 g/kWh (Umweltbundesamt 2015); CO_2^{eq} of district heat (from fossil energy carriers): 325 g/kWh (Umweltbundesamt 2013).

6.2 Simulation of Module Assembly

In this second case study, a simulation model was created for the assembly of battery modules. This demonstration focused the application of the multiscale core model for the evaluation of different process chain configurations. For simplification, only the process chain scale with workstations[15] was examined neglecting processes, workers, TBS, and the building. Due to this specific focus, this section does not specifically cover each step of the application procedure.

Problem Formulation and Objective Definition

The scope of this study was the comparison of a traditional assembly line configuration with a matrix-structured process chain layout for the simultaneous assembly of three exemplary types of battery modules. These modules differ regarding the number of cells, installed cables and sensors, geometric dimensions, and the housing. Consequently, although the production steps of all considered module types are in general identical, there are differences in the exact production steps and related processing times. In this case, two module types require eight production steps while the third requires seven steps because it does not contain a cooling system. Table 6.3 lists the production steps with related processing times for the three module types.[16]

The differing processing times of production steps result in starving and blocking of workstations. Thus, the goal of the production planning is defining process chain layouts and machine allocations which enable a high system utilization by avoiding starving and blocking. The objective of the simulation study was testing of different process chain layouts, different buffer sizes of workstations, and different allocations of production steps to workstations.

Table 6.3 Production steps with related processing times for each module type

	Processing time per production step (min)							
	PS_1	PS_2	PS_3	PS_4	PS_5	PS_6	PS_7	PS_8
Module type 1	3	5	7	5	4	5	6	5
Module type 2	4	6	8.5	6.3	4	6	6	5
Module type 3	2.5	4.5	5	3	5	–	5	5

[15] In this case study, the term workstation was used since assembly tasks are often manual tasks which are supported by different tools or resources.

[16] The processing times are defined based on assumptions and serve the purpose of demonstration. They do not reflect real-word production data.

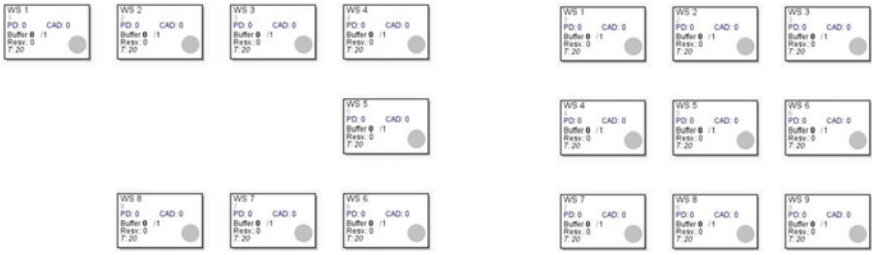

(a) assembly line configuration **(b)** matrix-structured configuration

Fig. 6.13 Screenshots of the assembly line configuration in u-shape (**a**) and the matrix-structured configuration (**b**) modeled in AnyLogic

Development of Models and Implementation

The multiscale core model was used for modeling of different process chain configurations and for evaluating scenarios regarding utilization and production time. In the model, the assembly line configuration and the matrix-structured configurations were created by specifying the workstation coordinates as well as the allocation of production steps to workstation. The operational states of workstations were represented by generic machine models. Energy demands were not observed in this study. Moreover, shift hours were not considered since TBS systems are not modeled and there are no effects of weather conditions on any production system element. Battery modules were represented by processing unit agents and the control strategy shortest throughput time was used to control the flow of processing units.

For the assembly line configuration, each production step was allocated to one workstation. Hence, in this case there were eight workstations which were positioned within the virtual shop floor coordinate system according to the order of production steps. Each workstation must have the required resources (e.g. tools).

For the matrix-structured configuration, each production step was allocated to multiple workstations based on different criteria. For example, if different production steps require the same tools (e.g. for fixation of cells on a base plate and for mounting of the housing), these production steps can be allocated to the same workstation. In this study, the production steps were allocated to nine workstations. Figure 6.13a, b present screenshots of the implemented process chains configurations.

Definition and Execution of Simulation Runs

The simulation model was used to determine the utilization and total production time for the assembly line and the matrix-structured configuration. For each configuration, the assembly of 500 modules was simulated in one simulation run with a random sequence of product types. The buffer size of each workstation was set to one. A fixed seed value was used for simulation in order to replicate the same sequence of products for each simulation run. This random sequence of product types should represent unknown demands for each product type. After the first two simulation

runs for both the line and matrix-structured configuration, a third run was executed to analyze an optimized matrix-structured configuration.

Evaluation of Simulation Results and Objectives

The results of the simulation runs were analyzed regarding the indicators utilization and overall production time for the simulated assembly of 500 modules. Figure 6.14 shows the plot of the utilization for the assembly line and matrix-structured configuration. The plots for both configurations show a fluctuation of the utilization which can be explained by regular starving and blocking of workstations. However, the utilization of the matrix-structured configuration (mean: 78.8%) is higher compared to the utilization of the assembly line configuration (mean: 69.5%). Moreover, the required production time for 500 modules is approximately 20% shorter with the matrix-structured configuration (including ramp-up and ramp-down of the assembly activity).

For further optimization of the matrix-structured configuration, the causes of blocking were investigated. A total of 186 blockings occurred during the simulation run. It was analyzed in which state a processing units could not be forwarded to a next workstation. A histogram was created showing the production step of processing units at which blocking occurred. This indicated which production steps were not sufficiently available in the process chain. Figure 6.15 presents the histogram which shows that processing units are often blocked after production step PS_4 and PS_7. Consequently, workstations for production step PS_5 and PS_8 were not available when needed. As a solution, these both production steps were additionally allocated to workstation 9. Another simulation run was executed to evaluate this change in production step allocations. Figure 6.16 presents the plot of the resulting utilization of the adjusted matrix-structured configuration in comparison to the previous simulation results of the initial matrix-structured configuration. The adjusted matrix-structured configuration resulted in a slightly higher utilization (mean: 81.6%) and a shorter production time. The total number of blockings was reduced to 49. This procedure

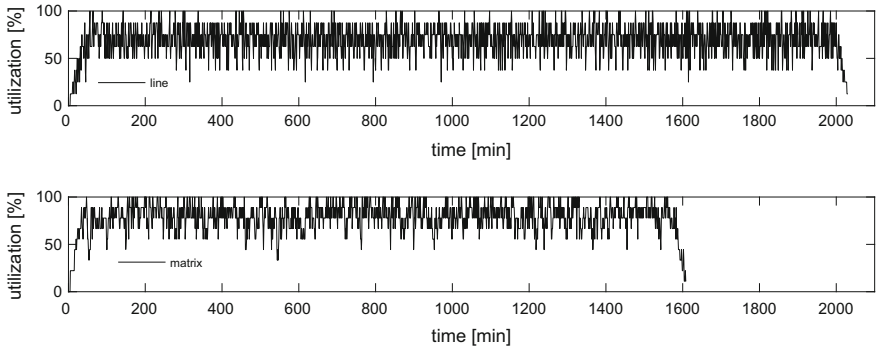

Fig. 6.14 Simulation results: Utilization of assembly line (*top*) and matrix-structured configuration (*bottom*)

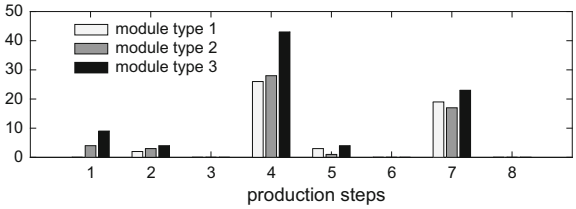

Fig. 6.15 Histogram of blockings per production step

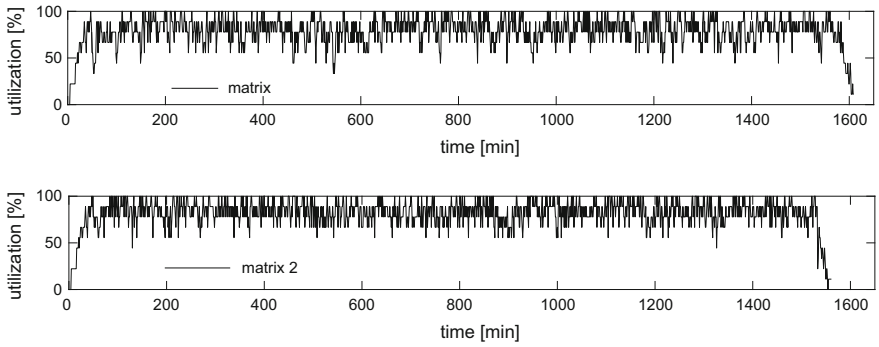

Fig. 6.16 Simulation results: Utilization of the initial (*top*) and the adjusted matrix-structured configuration (*bottom*)

for analyzing blockings could be repeated in order to further optimize the allocation of production steps. Alternatively to the additional allocation of production steps to other workstations, buffer sizes may be increased or new workstations added to the assembly system. The effects of such improvement measures can be analyzed with the simulation model.

The core model could also be configured for the consideration of machine failures. Probability distribution could be used to model the times between the occurrence of machine failures (MTTF) and until failures are repaired (MTTR). The model must be used to execute a large number of simulation runs with random seed value in order to address the implemented stochastic effects and to avoid a snap-shot character of simulation results. It was shown in Schönemann et al. (2015) that matrix-structured assembly systems can be more suitable for handling stochastic machine failures in comparison to sequential assembly lines. In the analyzed scenario, an assembly line configuration was compared to a matrix-structured configuration. The failure behavior of each machine was specified by Weibull functions for MTTF and uniform distributions for MTTR. Weibull functions have been used since they are adjustable to individual machine behavior. The uniform distribution allowed to equally consider short and long repair times. The model was used to execute 100 simulation runs with random seed values of the random number generator. The results show a higher

utilization of the matrix-structured configuration which was equally high compared to the deterministic case without machine failures.

In summary, this second case study has shown how the process chain model can be used to evaluate different process chain configurations. The shown evaluation addressed the economic performance of an assembly system by analyzing the system utilization and the production time for a predefined yield. Such analysis of the process chain performance may also be applied to cell production in the case that multiple redundant machines are available. Moreover, in further simulation runs, an modeled process chain of an assembly system can also be embedded within a factory environment and extended by detailed models for processes, TBS, and the building – similar to the demonstration in the first case study.

References

T. Baines, S. Mason, P. O. Siebers, and J. Ladbrook. Humans: The missing link in manufacturing simulation? *Simul. Model. Pract. Theory*, 12(7-8 SPEC. ISS.):515–526, 2004. ISSN 1569190X. doi:10.1016/S1569-190X(03)00094-7.

DWD. Testreferenzjahre (TRY) (web page, accessed 2016-03-28), 2016. URL http://www.dwd.de/DE/klimaumwelt/klimaforschung/spez_themen/try/try_node.html.

G. Posselt. *Towards Energy Transparent Factories*. Sustainable Production, Life Cycle Engineering and Management. Springer International Publishing, 2016. ISBN 978-3-319-20868-8. doi:10.1007/978-3-319-20869-5.

M. Schönemann, P. Greschke, C. Herrmann, and S. Thiede. Simulation of matrix-structured manufacturing systems. *J. Manuf. Syst.*, 37:104–112, 2015. doi:10.1016/j.jmsy.2015.09.002.

Umweltbundesamt. Emissionsbilanz erneuerbarer Energieträger - Bestimmung der vermiedenen Emissionen im Jahr 2012 (Emission balance of renewable energies - determination of avoided emissions in 2012), 2013.

Umweltbundesamt. Entwicklung der spezifischen Kohlendioxid- Emissionen des deutschen Strommix in den Jahren 1990 bis 2014, 2015.